Colloids and Surfaces B: Biointerfaces 99 (2012) 38–44

Contents lists available at SciVerse ScienceDirect

Colloids and Surfaces B: Biointerfaces

journal homepage: www.elsevier.com/locate/colsurfb

Dual crosslinked hydrogel nanoparticles by nanogel bottom-up method for sustained-release delivery

Asako Shimoda[a], Shin-ichi Sawada[d], Arihiro Kano[b], Atsushi Maruyama[b], Alexandre Moquin[c], Françoise M. Winnik[c], Kazunari Akiyoshi[a,d,*]

[a] Institute of Biomaterials and Bioengineering, Tokyo Medical and Dental University, 2-3-10 Kanda-Surugadai, Chiyoda-ku, Tokyo 101-0062, Japan
[b] Institute for Materials Chemistry and Engineering, Kyushu University, 744 Motooka, Nishi-ku, Fukuoka 819-0395, Japan
[c] Faculty of Pharmacy and Department of Chemistry, Universite de Montreal, CP 6128 Succursale Centre Ville, Montreal QC H3C 3J7, Canada
[d] Department of Polymer Chemistry, Graduate School of Engineering, Kyoto University, Katsura, Nishikyo-ku, Kyoto, 615-8510, Japan

ARTICLE INFO

Article history:
Available online 19 September 2011

Keywords:
Nanogel
Polysaccharide
Sustained drug delivery
Hydrogel
Biodegradable
Asymmetrical flow field-flow fractionation

ABSTRACT

Polysaccharide–PEG hybrid nanogels (CHPOA–PEGSH) crosslinked by both covalent ester bonds and physical interactions were prepared by the reaction of a thiol-modified poly(ethylene glycol) (PEGSH) with acryloyl-modified cholesterol-bearing pullulan (CHPOA). Experimental parameters, including CHPOA concentration, the degree of acryloyl substitution of CHPOA, and the initial amounts of CHPOA and PEGSH, were modified in order to assess their effect on the size of the nanogels (50–150 nm) and on their degradation kinetics, monitored by dynamic light scattering (DLS) and asymmetrical flow field-flow fractionation (AF4) chromatography. Rhodamine-labeled nanogels were injected intravenously into mice and their concentration in blood was determined by a fluorescence assay as a function of post-injection time. The elimination half-life ($t_{1/2}$) of CHPOA–PEGSH nanoparticles was about 15-fold longer (18 h) than that of CHP nanogels (1.2 h). The half-life enhancement of CHPOA–PEGSH was attributed to the presence of the crosslinker PEG chains, which prevent non-specific protein adsorption, and to the slow hydrolysis kinetics of the crosslinking esters in the biological milieu. The hybrid CHPOA–PEGSH nanogels are expected to be useful as injectable nanocarriers for drugs and proteins, in view of their low surface fouling and slow hydrolysis rate.

1. Introduction

Nanometer-sized polymer hydrogel particles (nanogels) have recently received much attention for biomedical applications such as drug delivery systems [1–4]. Chemically crosslinked nanogels are usually prepared by nanoemulsion polymerization or by chemical crosslinking of the hydrophilic or hydrophobic polymer chains in polymer micelles [5–7]. We reported a new method of preparation of physically crosslinked nanogels formed by amphiphilic derivatives of the neutral polysaccharide pullulan, such as pullulans bearing low levels of cholesteryl groups (CHP), upon simple self-assembly in dilute aqueous solution [8]. The nanogels were shown to prevent the massive aggregation of proteins that typically occurs upon rapid removal of urea from solution of unfolded proteins. The enhanced yield of correct protein folding was ascribed to the hydrophobic binding of CHP with proteins, which in turn slows down the kinetics of protein aggregation [9,10].

In this fashion, CHP nanogels have been used to encapsulate in a transient fashion proteins, such as insulin [11], interleukin-12 (IL-12) [12], antigen proteins for cancer vaccine [13,14], and nasal vaccine [15]. Recombinant murine IL-12 (rmIL-12) was successfully incorporated in CHP nanogel simply by incubating rmIL-12 with nanogels. Subcutaneous injection into mice of CHP/rmIL-12/nanogel complexes resulted in a prolonged elevation of rmIL-12 concentration in the serum. However, the kinetics of drug level in serum was the same following intravenous or intraperitoneal injections of CHP/rmIL-12 nanogels as those recorded upon injection of a rmIL-12 solution used as a control. This observation was taken as an indication of the poor stability of CHP nanogels in the bloodstream, presumably due to the fact that nanogels are held together exclusively by physical forces without any covalent crosslinkers. Consequently, they rapidly release their cargo in blood following displacement of the therapeutic protein by plasma proteins.

To overcome the instability of physically crosslinked nanogel in vivo, we devised a means to strengthen nanogels by chemical crosslinking of the nanogels with polyethylene glycol (PEG)

* Corresponding author at: Department of Polymer Chemistry, Graduate School of Engineering, Kyoto University, Katsura, Nishikyo-ku, Kyoto, 615-8510, Japan. Tel.: +81 75 383 2589; fax: +81 75 383 2590.
E-mail address: akiyoshi@bio.polym.kyoto-u.ac.jp (K. Akiyoshi).

0927-7765/$ – see front matter © 2011 Elsevier B.V. All rights reserved.
doi:10.1016/j.colsurfb.2011.09.025

derivatives and coating the surface of nanogels with PEG. Acryloyl group-modified CHP nanogels were crosslinked by thiol group-modified four-armed polyethylene glycol (PEGSH) in water, thus forming nanogel-assembly like "raspberry-like" nanoparticles [16]. In the previous article, we reported the stability and sustained release of the nanogels assemblies upon subcutaneous injection in mice. We assess here the stability of PEG-crosslinked nanogels in blood serum and blood both in vitro and in vivo, following intravenous injection in mice. The nanogels assemblies were analyzed by asymmetrical flow field-flow fractionation with combined multiangle light scattering and dynamic light scattering detection coupled to UV–vis absorption detection, to assess, respectively, the concentration and the hydrodynamic size of the nanogels.

2. Experimental

2.1. Materials

Water was deionized using a Milli-Q water purification system (Millipore, Bedford, MA). Pentaerythritol tetra(mercaptoethyl) polyoxyethylene (PEGSH, Mw = 1.0×10^4 g mol^{-1}) was purchased from NOF Co. (Tokyo, Japan). Di-*n*-butyltin (IV) dilaurate (DBTDL), cysteine hydrochloride monohydrate, and 5,5′-dithio-*bis*-(2-nitrobenzoic acid) (DTNB) were purchased from Wako Pure Chemical Industries, Ltd. (Osaka, Japan). Fetal bovine serum (FBS) and minimum essential medium (MEM) were obtained from Invitrogen (Carlsbad, CA). 2-(Acryloyloxy) ethyl isocyanate (AOI) was purchased from Showa Denko Co (Tokyo, Japan). The cholesteryl pullulan nanogel sample (CHP, 1.2 cholesteryl groups per 100 glucose units) was synthesized as previously reported [17].

2.2. Dynamic light scattering (DLS)

The hydrodynamic diameters of the nanogels were determined by dynamic light scattering (DLS; Zetasizer Nano; Malvern, UK). The scattering angle was kept at 137° and the wavelength was set at 633 nm. The CHPOA nanogel concentration ranged from 1.0 to 5.0 mg mL^{-1}.

2.3. Asymmetrical flow field-flow fractionation (AF4)

Asymmetric flow field-flow fractionation was performed using an AF4 system (AFx2000MT, Postnova Analytics, Landsberg, Germany) combined with an UV/vis detector (SPD-20A, Postnova Analytics), a multiangle light scattering detector (MALS, Dawn 8+, Wyatt Technology), and a dynamic light scattering detector (Wyatt-QELS, Wyatt Technology). The channel had a thickness of 350 μm and was fitted with a regenerated cellulose membrane (10 kDa cut off, Z-MEM-AQU-631, RC, Postnova Analytics). The carrier medium was prefiltered (0.1 μm) phosphate buffered saline (pH 7.4). The sample was injected with a flow rate of 0.2 mL/min, followed by a 4 min-focusing with a cross-flow rate of 1.8 mL/min and a detector flow rate of 0.52 mL/min. Following a 1 min transition, a three-step cross-flow rate gradient was initiated for the elution mode. The starting cross-flow rate (1.8 mL/min) was kept constant for 8 min. It was decreased linearly to 0 mL/min within 10 min, and kept constant at 0 mL/min for 15 min to allow elution of the nanogels or assemblies of nanogels. The detector flow rate was kept at 0.52 mL/min throughout. The detection of the eluted nanogels was performed sequentially by UV absorbance at 556 nm (ε_{556} = 1411 mmol g^{-1} cm^{-1}, determined using a calibration curve), fluorescence with λ_{ex} 468 nm and λ_{em} 581 nm, multiangle light scattering (MALS) and DLS. Each fractogram presented is representative of a triplicate sample.

2.4. Synthesis of the nanogels

The CHPOA nanogels having 5, 19 or 23 acryloyl groups per 100 glucose units were prepared starting from a CHP sample (1.0 g, 6.2 mmol of anhydrous glucose units) dried under vacuum for 2 days at 70 °C before use. The CHP was dissolved under nitrogen in 50 mL of anhydrous dimethyl sulfoxide (50 mL, DMSO) at 45 °C. DBTDL (53, 201 or 242 μL; 90, 340 or 410 μmol) and AOI (42, 155 or 181 μL; 0.3, 1.2 or 1.4 mmol) were added to the CHP solution. The resulting mixture was kept in the dark for 24 h at 45 °C. The reaction mixture was subjected to repeated precipitations into ether/ethanol solution (ether >80% v/v). The isolated solid material was suspended in DMSO, dialyzed against deionized water, and isolated by lyophilization. The degree of substitution of acryloyl groups was determined from the ^{1}H NMR (500 MHz, DMSO-d6/D_2O: δ (ppm) 0.6–2.4 (cholesterol); 3.1–4.0 (glucose 2H, 3H, 4H, 5H, 6H); 4.7 (glucose 1H (1 → 6)); 4.9–5.1 (glucose 1H (1 → 4)); 5.9–6.3 (olefinic protons of the acryloyl group $-CH{=}CH_2-$). Rhodamine-labeled CHPOA (CHPOA–Rh) nanogels were synthesized as reported previously [18]. The degree of labeling was determined by UV/vis analysis at 556 nm (UV-1650PC, Shimadzu, Japan).

2.5. Preparation of CHPOA–PEGSH nanoparticles

To prepare CHPOA–PEGSH nanoparticles, samples of CHPOA nanogel (8 mg) in a PBS buffer (1 mL, pH 7.4) were treated with PEGSH in amounts such that the acryloyl group:thiol group molar ratios were 1:1, 2:1 and 4:1. The mixtures were kept at 37 °C for 24 h. Micrographs of CHPOA nanogels and CHPOA–PEGSH nanoparticles were obtained by freeze–fracture TEM (FF-TEM, JEM-1011, JEOL, Tokyo, Japan) at an accelerating voltage 100 kV. The sample was prepared using the aqueous solution of CHPOA nanogel or CHPOA–PEGSH nanoparticles containing 30% glycerol. The concentration of nanogel was 4 mg mL^{-1}, and the acryloyl:thiol molar ratio was 2:1 or 4:1. CHPOA–PEGSH nanogels were isolated in the dry form by lyophilization after 24 h incubation in PBS. Freeze-dried samples were resuspended in deionized water.

The thiol content of CHPOA–PEGSH nanoparticles was determined using Ellman's reagent [19]. CHPOA–PEGSH (4.0 mg mL^{-1}, obtained from acryloyl group:thiol group molar ratios of 1:1, 2:1 and 4:1) were dissolved in PBS. The nanoparticle solution (250 μL) was added to a mixture of the reaction buffer (2.5 mL, 0.1 M sodium phosphate, pH 8.0, containing 1 mM EDTA) and of Ellman's reagent solution (50 μL, 4.0 mg Ellman's Reagent in 1 mL reaction buffer). The mixture was kept at room temperature for 15 min prior to analysis. The SH concentration of the solutions was determined from their absorbance at 412 nm using a calibration curve obtained from cysteine–HCl. The degradation of CHPOA–PEGSH nanoparticles was monitored by ^{1}H NMR spectroscopy for samples incubated in PBS containing D_2O for 24 h at 37 °C. The level of nanoparticle degradation was estimated from the increase in the signal at 2.36 ppm, attributed to the protons in the Fig. S2 [20]. The stability of the nanogels in serum was monitored using 500 μL of CHPOA nanogels or CHPOA–PEGSH nanoparticles (acryloyl:thiol = 1:1, 2:1 or 4:1) solutions in MEM (2.0 mg mL^{-1}, 500 μL). The mixtures were incubated at 37 °C with 5% (v/v) FBS for different times. The resulting solution was analyzed by DLS in order to determine the hydrodynamic sizes of the nanoparticles.

2.6. Blood clearance measurements

The animal experiments were carried out under the guidance of the Animal Care and Use Committee, Kyushu, University. Seven-week-old Balb/c mice purchased from Kyudo Co., Ltd. (Tosu, Japan) were treated with suspensions of CHP–Rh or CHPOA–Rh–PEGSH

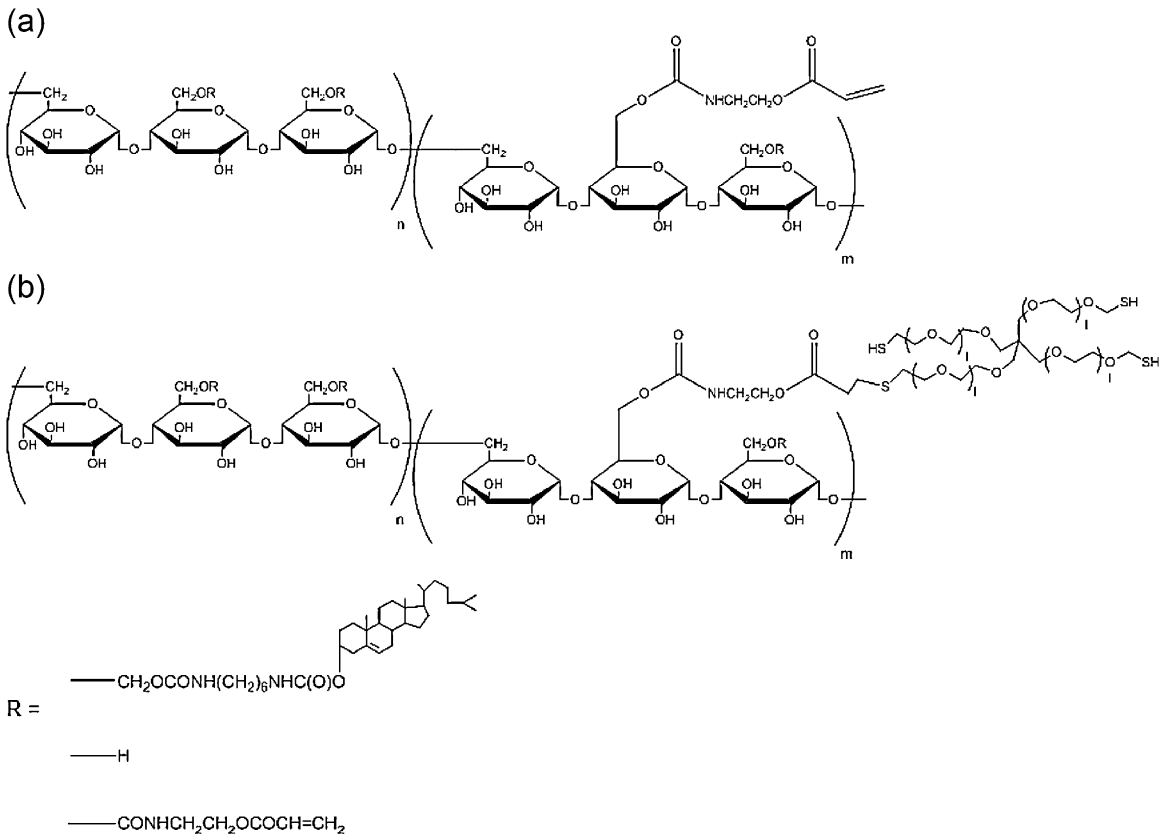

Fig. 1. Chemical structures of (a) CHPOA nanogel and (b) CHPOA–PEGSH nanoparticle.

(acryloyl:thiol = 2:1 or 4:1) in PBS (100 μL 4 mg mL^{-1}) by injection into a tail vein. At various time intervals, blood was collected with a hematocrit tube from the orbital sinus. The blood samples were mixed with a solution of EDTA (1.0 μL, 0.5 M) in PBS and centrifuged for 5 min at 10,000 rpm. The supernatant was diluted with PBS. The fluorescence intensity of the supernatant was determined upon excitation at 550 nm using a Wallac ARVOSX 1420 Multilabel Counter. The total blood volume was calculated as 0.08 mL g^{-1} body weight. The pharmacokinetic parameters were analyzed with a non-compartmental model using WinNonlin (4.0 software; Pharsight Corporation, Mountain View, CA).

3. Results and discussion

3.1. Synthesis and crosslinking of acryloyl CHP nanogels (CHPOA)

The synthesis of CHPOA is outlined in Fig. 1. It involves the reaction of 2-(acryloyloxy) ethyl isocyanate with hydroxyl groups of CHP using di-*n*-butyl-tin (IV) dilaurate as a catalyst. The reaction takes place under mild conditions and provides excellent control over the degree of modification of the nanogels. ^{1}H NMR spectroscopy analysis of CHPOA samples in DMSO-d6/D_2O confirmed that the level of acryloyl group incorporation was nearly identical to the initial feed (Fig. S1). In previous studies [16], acryloyl CHP nanogels were obtained by esterification of CHP hydroxyl groups with acrylic acid in the presence of N,N-dicyclohexylcarbodiimide (DCC). Although, the transformation took place, the esterification yield was low, leading to difficulties in adjusting the level of acryloyl group incorporation. Moreover, the urea that is formed as a by-product of the synthesis, could not be removed readily. The new synthesis reported here, which overcomes these difficulties, is a significant improvement over other synthetic routes.

Three batches of CHPOA were prepared, setting the initial ratio of AOI per glucose unit to 5, 19 or 23. The modified CHP samples were purified thoroughly to remove the catalyst prior to further transformation. Their hydrodynamic diameter measured by dynamic light scattering for suspensions (1.0 mg mL^{-1}) in PBS at pH 7.4, decreased as follows, with increasing OA incorporation: CHPOA5, 53.7 ± 1.8 nm; CHPOA19, 43.3 ± 1.0 nm; and CHPOA23, 30.6 ± 0.4 nm. Asymmetrical flow field-flow fractionation analysis of the CHPOA samples confirmed that the mean molecular weight (Mw) of single CHPOA23 nanogels was 9.7 × 10^5 g mol^{-1}, as determined from fractograms monitored by MALS (Fig. 2). Hence, the number of CHPOA molecules per nanogel was 8–9. This value is larger that the number of CHP molecules (4–5) associated in CHP nanogels nanoparticle consisting of approximately 4–5 CHP molecules [21]. The increase of the number of associated CHPOA molecules and the enhanced size of CHPOA nanogels, compared to CHP nanogels, may be attributed to the presence of the hydrophobic acryloyl groups.

Several experimental parameters affecting the outcome of the Michael addition of PEGSH to the acryloyl groups of CHPOA were examined in order to provide guidelines to control the properties of the resulting crosslinked CHPOA–PEGSH nanogels. First, reactions were conducted with solutions of increasing CHPOA concentration (1.0–10 mg mL^{-1}), keeping the acryloyl:thiol molar ratio set at 1:1. All syntheses were carried out at 37 °C for 24 h. The size of the nanogels was monitored by DLS analysis of aliquots taken from the mixture at specific times during the reaction. It increased rapidly over the first two hours and leveled off to a constant value after 24 h. The ultimate sizes of the crosslinked nanogels, as well as the size distribution, depend on the initial CHPOA concentration. For instance crosslinking of CHPOA23 led to nanogels with hydrodynamic diameters of 53.5 ± 0.1 nm (1 mg mL^{-1}) and 142.7 ± 3.7 nm (5 mg mL^{-1}) and polydispersity indices (PDI) of 0.163 (1 mg mL^{-1})

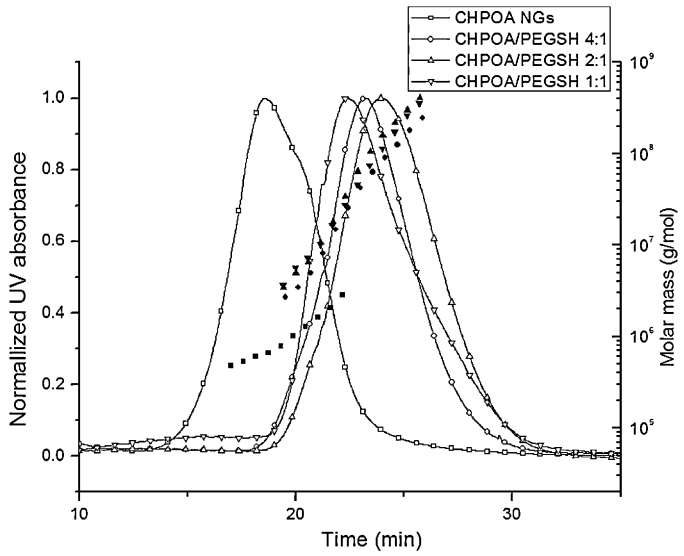

Fig. 2. AF4 fractograms of CHPOA–rhodamine and CHPOA–PEGSH-rhodamine raspberry like nanogels. The lines and the unconnected dots represent, respectively, the normalized UV absorbance at 556 nm and the molar masses of the nanogels as function of the elution time. The separation is based on the diffusion coefficient of the particles.

and 0.463 (5 mg mL^{-1}). Further increase in size and PDI of the crosslinked nanogels was observed when the CHPOA concentration exceeded 5 mg mL^{-1}. Viscous gels formed when the initial CHPOA was 10 mg mL^{-1} or higher, signaling the occurrence of second-order micro/macro gelation due to the crosslinking of preformed raspberry nanogels (Fig. 3).

Second, we set the initial CHPOA concentration at 4 mg mL^{-1} and assessed the effect of the acryloyl/thiol molar ratio on the outcome of the crosslinking reaction. This set of measurements was carried out starting from CHPOA23. The acryloyl:thiol molar ratios were 1:1, 2:1, and 4:1. The resulting nanogels were

Table 1
The diameter of CHPOA–PEGSH nanoparticles.

Molar ratio (acryloyl:thiol)	Diameter (nm)	PdI
1:1	108.7 ± 1.7	0.291 ± 0.013
2:1	117.5 ± 1.5	0.290 ± 0.002
4:1	78.0 ± 0.8	0.244 ± 0.001

Nanogel concentration: 4 mg mL^{-1}

Table 2
The diameter of CHPOA–PEGSH nanoparticles before and after freeze-dry.

Sample	Before	After
	Diameter (nm)	Diameter (nm)
CHPOA23–PEGSH 1:1	113.0 ± 4.3	Gel
CHPOA23–PEGSH 2:1	121.7 ± 4.5	Gel
CHPOA23–PEGSH 4:1	87.3 ± 7.4	71.1 ± 2.9

Nanogel concentration: 4 mg mL^{-1}

analyzed by DLS and by a colorimetric assay with Ellman's reagent for quantitative determination of the unreacted thiol groups. The hydrodynamic diameter of the nanogels ranged from 80 to 120 nm with increasing acryloyl:thiol molar ratio (Table 1), while the free thiol ratios in the CHPOA23–PEGSH nanoparticles were 34.5 ± 2.5%, 8.2 ± 2.3%, and 1.6 ± 1.9% of the total thiol concentration, respectively, with initial acryloyl/thiol ratios of 1:1, 2:1 and 4:1. The residual amounts of acryloyl groups of nanogel after the reaction with PEGSH were estimated by using ^{1}H NMR. The percentage of the residual acryloyl groups in the CHPOA23-PEGSH nanoparticles were 0%, 58%, and 68%, with initial acryloyl/thiol ratios of 1:1, 2:1 and 4:1, respectively. The residual thiol groups and acryloyl groups bound to the nanogels will be useful to prepare functional nanoparticles carrying ligands such as peptides or antibodies. We observed however that when nanoparticles bearing more than ~8% SH were freeze-dried, rehydration resulted in irreversible gelation via disulfide formation. In contrast the nanoparticles with ~2% free SH or less readily redispersed in deionized water after freeze drying (Table 2).

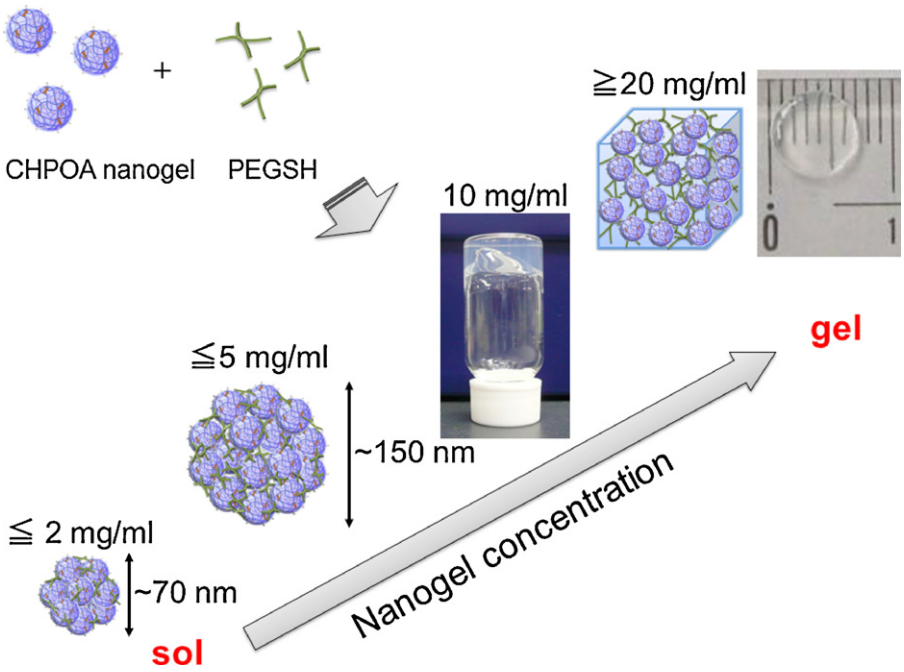

Fig. 3. Hierarchical structure of CHPOA–PEGSH hydrogel. Under dilute conditions, CHPOA–PEGSH forms nanoparticles around 150 nm in diameter. Under higher concentrations, CHPOA–PEGSH forms macrogels. Nanogel crosslinked nanoparticles can be used for injectable materials, and macrogels can be used as scaffolds for tissue engineering.

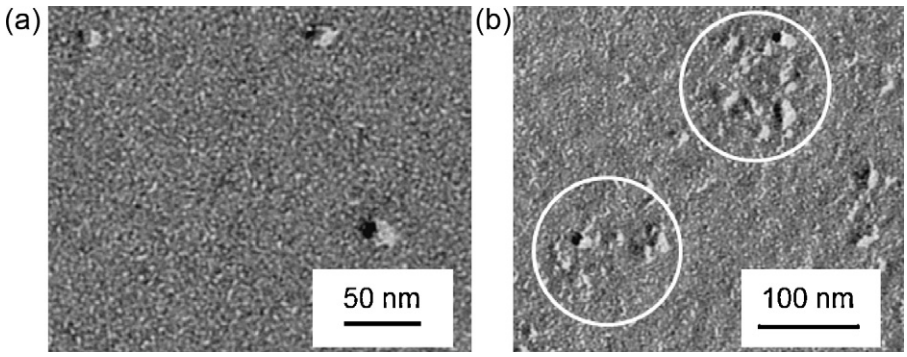

Fig. 4. TEM images of (a) CHPOA nanogels and (b) CHPOA–PEGSH nanoparticles. The nanogel concentration was 4 mg mL^{-1}. The molar ratio of acryloyl/thiol was 2:1.

Crosslinked nanogels obtained from CHPOA23 (4 mg mL^{-1}) and PEGSH (acryloyl/thiol molar ratios 4:1, 2:1 and 1:1) were analyzed by AF4 (Table S1). The fractograms of each sample presented a broad band eluting at longer times, compared to the initial nanogels. This increase in elution time, together with the absence of signal at shorter times, confirm that crosslinking of isolated nanogels occurred with high yield. The size distribution of the crosslinked nanogel was significantly broader than that of the starting CHPOA23 nanogels, revealing some level of heterogeneity in their composition. Under these reaction conditions, both inter- and intra-nanogel crosslinking can occur. When the acryloyl/thiol molar ratio is 1:1, i.e. the CHPOA concentration is high relative to the PEGSH concentration, inter-nanogel crosslinking reactions are most efficient, leading to relatively large crosslinked nanogels. In contrast, when the reaction is carried under conditions of higher PEGSH concentration (acryloyl/thiol is 4:1), intra-nanogel crosslinking reaction predominate, due to dilute conditions of PEGSH. As a result, the size of the resulting particles was smaller than that in the case of acryloyl/thiol = 1:1. The size of the nanoparticle is determined by the balance of concentration of nanogel and PEGSH as a crosslinker.

3.2. Structure of the crosslinked nanogels

The "raspberry-like" morphology of the crosslinked nanogels was confirmed by transmission electron microscopy imaging of freeze-fractured specimens of CHPOA23–PEGSH embedded in frozen 30% glycerol. Micrographs of a CHPOA23–PEGSH (acryloyl/thiol: 2/1) sample and of the original nanogel are presented in Fig. 4. Clusters of closely associated individual nanogels are seen readily in Fig. 4b, corresponding to the crosslinked sample. In contrast (Fig. 4a), the micrograph of the initial nanogel features only well separated nanogels, with no sign of clustering or aggregation.

To confirm the covalent nature of the inter-nanogel crosslinking we carried out a physico-chemical test, which consisted in treating samples of CHPOA–PEGSH suspensions with methyl-β-cyclodextrin, (Me-β-CD) a complexing agent of cholesterol. Treatment of CHP suspensions with Me-β-CD triggers the unraveling of the nanogels as a consequence of the disruption of the hydrophobic cholesteryl clusters due to preferential interaction of isolated cholesteryl groups with Me-β-CD. In contrast, the addition of Me-β-CD to a suspension of CHPOA–PEGSH nanogels resulted in the swelling of the nanoparticles, by a factor of ~20–30% in volume (Table 3). The increase in size of the nanoparticles reflects the increase in the size of the nanogel units (building blocks) as a result of the destruction of the physical crosslinking points by complexation of cholesteryl groups and Me-β-CD, coupled with the fact that disintegrated nanogels have to remain part of the larger object as a result of the chemical crosslinking, unaffected by the addition of Me-β-CD. A pictorial representation of the swelling mechanism is given in Fig. 5. Me-β-CD-loaded nanoparticles are currently investigated building blocks in the construction of cyclodextrin-based supramolecular nano-architectures [22–24]. The complex formed between Me-β-CD and CHPOA–PEGSH may be of use as new supramolecular materials such as artificial chaperones.

Table 3
The diameter change of CHPOA–PEGSH nanoparticles before and after Me-β-CD addition.

Sample	Acryloyl:Thiol	Before	After
		Diameter (nm)	Diameter (nm)
CHPOA23–PEGSH	1:1	108.7 ± 1.7	131.5 ± 0.5
	2:1	117.5 ± 1.5	143.5 ± 4.5
	4:1	78.0 ± 0.8	86.0 ± 0.4

Nanogel concentration: 4 mg mL^{-1}

3.3. Degradation of crosslinked nanogels under physiological conditions

As seen in Fig. 1, the synthetic route selected involves the formation of an ester function linking pullulan chains to the PEGSH crosslinker. This functional group was chosen specifically in view of its ability to undergo hydrolysis at pH 7.4, hence allowing slow disruption of the crosslinked nanogel network and reversal to isolated units. To confirm that hydrolysis of the ester group takes place within the nanogel construct, CHPOA–PEGSH of various composition were exposed to a pH 7.4 phosphate buffer at 37 °C for over 1 month. During this incubation time, they were analyzed repeatedly by ^{1}H NMR spectroscopy in order to detect changes in the intensity of the signal at 2.36 ppm, attributed to the ester hydrolysis (Fig. S2). The percent hydrolysis recovered from this ^{1}H NMR analysis was plotted as a function of time for three different CHPOA–PEGSH nanoparticles (Fig. 6a). Hydrolysis reached levels of ~25–50% after 10 days and gradually leveled off.

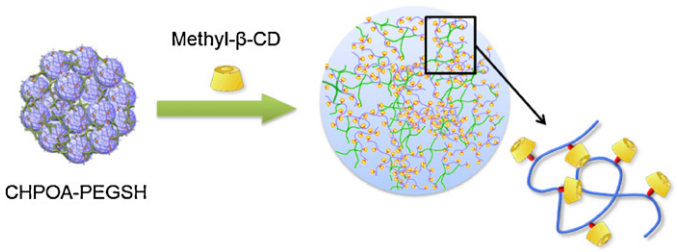

Fig. 5. Methyl-β-CD responding swelling behavior.

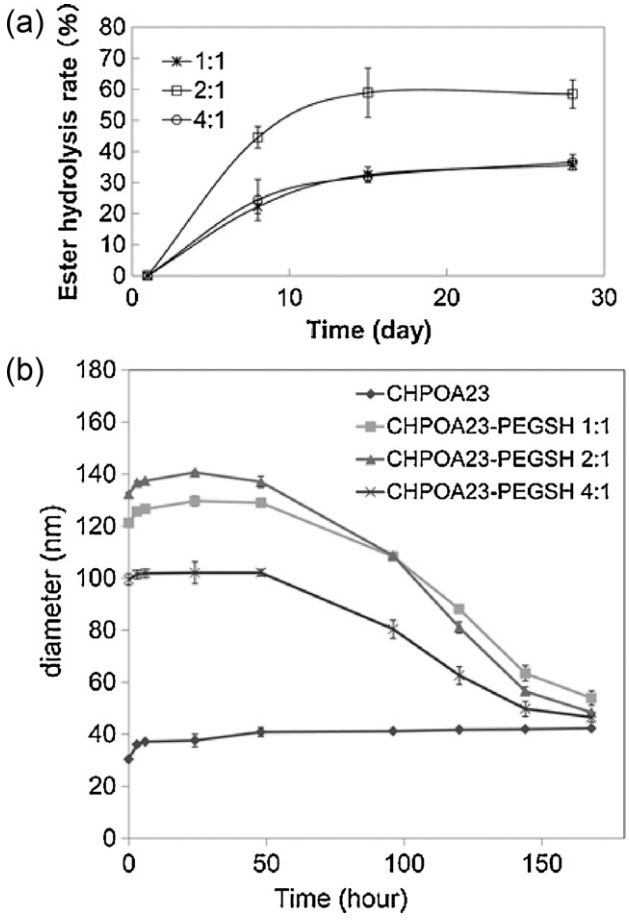

Fig. 6. (a) The ester hydrolysis of CHPOA–PEGSH nanoparticles. Final nanogel concentration was 4 mg mL^{-1}, the molar ratio of acryloyl/thiol was 1:1, 2:1 and 4:1. The data represent mean ± standard deviation (SD), $n = 3$. (b) Stability of CHPOA nanogel (♦) and CHPOA–PEGSH nanoparticles (acryloyl:thiol = 1:1 (■), 2:1(▲) and 4:1 (×)) in the presence of 5% FBS. The data represent mean ± standard deviation (SD), $n = 3$.

We monitored also the fate of crosslinked nanogels incubated in serum at 37 °C. The extent of ester hydrolysis could not be measured by ^{1}H NMR, due to the complexity of the incubation medium. Instead, we recorded by DLS the changes in the hydrodynamic size of the nanoparticles as a function of incubation time (Fig. 6b). The hydrodynamic diameters were constant for 2 days, then, they decreased with time reaching the value of the diameter of the initial nanogel (~40 nm) after 1 week. These results suggest that the hydrolysis of the ester bonds between the CHPOA nanogel and PEGSH was catalyzed by serum esterases [25,26], resulting in the gradual release of nanogels from the crosslinked constructs.

3.4. Blood clearance of crosslinked nanogels following intravenous injection in mice

Suspensions of rhodamine-labeled CHP nanogels and CHPOA–PEGSH nanogels in PBS were injected intravenously in mice followed by blood sampling and analysis after regular time periods, in order to determine the concentration of rhodamine-labeled nanoparticles in blood. The results of the experiments performed with CHP nanogel and two types of crosslinked nanogels are plotted in Fig. 7 as the percent of the injected nanogel concentration remaining in the blood as a function of post-injection time. CHP nanogels were eliminated from the blood within 6 h, whereas the CHPOA–PEGSH nanogels had a significantly longer circulation time: approximately 40–50% of the nanoparticles remained in circulation 6 h following injection and, after 24 h, 20–30% of the

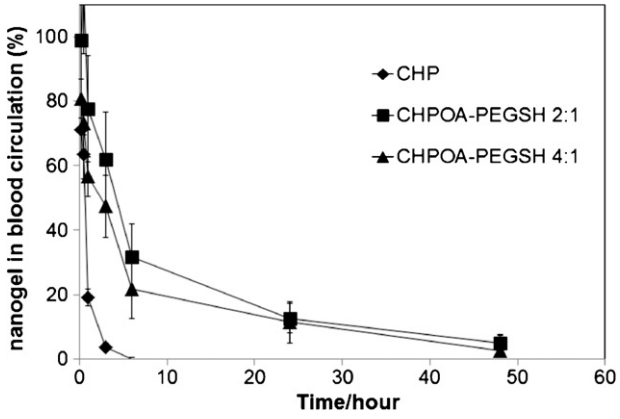

Fig. 7. Blood circulation of CHP nanogel (♦) and CHPOA–PEGSH (acryloyl:thiol = 2:1 (■), 4:1 (▲)). The data represent mean ± standard deviation (SD), $n = 4$.

nanoparticles remained in the blood. A pharmacokinetic analysis of the data revealed that the half-life ($t_{1/2}$) of CHPOA–PEGSH nanoparticles (2:1, 18.0 h; 4:1, 15.5 h) was about 15-fold greater than that of CHP nanogels (1.2 h).

The long circulation in blood is one of the most important issues to achieve effective cancer chemotherapy in intravenous drug delivery system. The superior performance of CHPOA–PEGSH nanogels, compared to CHP nanogels, can be attributed to several effects acting in concert: (1) structural stabilization provided by the covalent crosslinks; (2) prevention of non-specific protein adsorption by the PEG fragments associated with the chemical crosslinkers [27–29]; and (3) controlled release of individual nanogel by sustained hydrolysis of the ester bond between the PEG crosslinker and the glucose units of the nanogel.

4. Conclusion

We designed nanoparticles comprising assemblies of CHPOA nanogel particles and thiol-modified polyethylene glycol. The size of the nanogel assemblies was controlled in the range 50–150 nm by varying the nanogel concentration, degree of substitution of acryloyl groups of CHPOA nanogels and acryloyl:thiol molar ratio. The elimination half-life ($t_{1/2}$) of CHPOA–PEGSH nanoparticles was much longer than that of CHP nanogels. Thus, the nanoparticles can be utilized as injectable nanocarriers capable of controlled release of proteins such as cytokines over relatively long periods. We are able to select various self-assembled nanogels as building blocks and prepare multi-functional naoparticles. The bottom-up nanogel fabrication method opens up a new field for creating tailor-made functional hydrogel materials.

Acknowledgements

This work was supported by a Grant-in-Aid for Scientific Research from the Ministry of Education, Culture, Sports, Science and Technology (No. 20240047 and 22114009). This work was performed under the Cooperative Research Program of Network Joint Research Center for Materials and Devices (Institute for Materials Chemistry and Engineering, Kyushu University).

Appendix A. Supplementary data

Supplementary data associated with this article can be found, in the online version, at doi:10.1016/j.colsurfb.2011.09.025.

References

[1] J.P. Rao, K.E. Geckeler, Prog. Polym. Sci. 36 (2011) 887.
[2] A.V. Kabanov, S.V. Vinogradov, Angew. Chem. Int. Ed. 48 (2009) 5418.
[3] A. Fernández-Barbero, I.J. Suárez, B. Sierra-Martín, A. Fernández-Nieves, F.J. de Las Nieves, M. Marquez, J. Rubio-Retama, E. López-Cabarcos, Adv. Colloid Interface Sci. 147–148 (2009) 88.
[4] Y. Sasaki, K. Akiyoshi, Chem. Rec. 10 (2010) 366.
[5] K. Nagahama, T. Ouchi, Y. Ohya, Macromol. Biosci. 8 (2008) 1044.
[6] M. Oishi, Y. Nagasaki, React. Funct. Polym. 67 (2007) 1311.
[7] E.S. Lee, D. Kim, Y.S. Youn, K.T. Oh, Y.H. Bae, Angew. Chem. Int. Ed. Engl. 47 (2008) 2418.
[8] K. Akiyoshi, S. Deguchi, T. Tajima, T. Nishikawa, J. Sunamoto, Macromolecules 30 (1997) 857.
[9] Y. Nomura, M. Ikeda, N. Yamaguchi, Y. Aoyama, K. Akiyoshi, FEBS Lett. 553 (2003) 271.
[10] N. Morimoto, T. Endo, Y. Iwasaki, K. Akiyoshi, Biomacromolecules 6 (2005) 1829.
[11] K. Akiyoshi, S. Kobayashi, S. Shichibe, D. Mix, M. Baudys, S.W. Kim, J. Sunamoto, J. Control. Release 54 (1998) 313.
[12] T. Shimizu, T. Kishida, U. Hasegawa, Y. Ueda, J. Imanishi, H. Yamagishi, K. Akiyoshi, E. Otsuji, O. Mazda, Biochem. Biophys. Res. Commun. 367 (2008) 330.
[13] Y. Ikuta, N. Katayama, L. Wang, T. Okugawa, Y. Takahashi, M. Schmitt, X. Gu, M. Watanabe, K. Akiyoshi, H. Nakamura, K. Kuribayashi, J. Sunamoto, H. Shiku, Blood 99 (2002) 3717.
[14] S. Kageyama, S. Kitano, M. Hirayama, Y. Nagata, H. Imai, T. Shiraishi, K. Akiyoshi, A.M. Scott, R. Murphy, E.W. Hoffman, L.J. Old, N. Katayama, H. Shiku, Cancer Sci. 99 (2008) 601.
[15] T. Nochi, Y. Yuki, H. Takahashi, S. Sawada, M. Mejima, T. Kohda, N. Harada, I.G. Kong, A. Sato, N. Kataoka, D. Tokuhara, S. Kurokawa, Y. Takahashi, H. Tsukada, S. Kozaki, K. Akiyoshi, H. Kiyono, Nat. Mater. 9 (2010) 572.
[16] U. Hasegawa, S. Sawada, T. Shimizu, T. Kishida, E. Otsuji, O. Mazda, K. Akiyoshi, J. Control. Release 140 (2009) 312.
[17] K. Akiyoshi, S. Deguchi, N. Moriguchi, S. Yamaguchi, J. Sunamoto, Macromolecules 26 (1993) 3062.
[18] H. Ayame, N. Morimoto, K. Akiyoshi, Bioconjug. Chem. 19 (2008) 882.
[19] I. Bravo-Osuna, D. Teutonico, S. Arpicco, C. Vauthier, G. Ponchel, Int. J. Pharm. 340 (2007) 173.
[20] A.E. Rydholm, K.S. Anseth, C.N. Bowman, Acta Biomater. 3 (2007) 449.
[21] K. Kuroda, K. Fujimoto, J. Sunamoto, K. Akiyoshi, Langmuir 18 (2002) 3780.
[22] R. Villalonga, R. Cao, A. Fragoso, Chem. Rev. 107 (2007) 3088.
[23] M.E. Davis, Mol. Pharm. 6 (2009) 659.
[24] F. Manakker, T. Vermonden, C.F. Nostrum, W.E. Hennink, Biomacromolecules 10 (2009) 3157.
[25] H. Xu, Y. Deng, D. Chen, W. Hong, Y. Lu, X. Dong, J. Control. Release 130 (2008) 238.
[26] B. Li, M. Sedlacek, I. Manohaban, R. Boopathy, E.G. Duysen, P. Masson, O. Lockridge, Biochem. Pharmacol. 7 (2005) 1673.
[27] R.L.C. Wang, H.J. Kreuzer, M.M. Grunze, J. Phys. Chem. B 101 (1997) 9767.
[28] D.L. Elbert, J.A. Hubbell, Chem. Biol. 5 (1998) 177.
[29] M.A. Cooper, Nat. Rev. Drug Discov. 1 (2002) 515.